Characterization of Corrugated Waveguides by Modal Analysis

Jaime Esteban and Jesús M. Rebollar

Abstract—**A general formulation for the characterization of corrugated waveguides is presented. The formulation is based on modal expansion in the different smooth-walled waveguides which constitute the corrugated structure and on the use of mode matching at discontinuities. The use of an admittance matrix formulation and a suitable root-finding algorithm leads to a rigorous and efficient technique. Dispersion curves are presented for corrugated waveguides of circular and rectangular cross sections. As predicted by other authors, complex modes have been obtained for deep corrugations. The effect of the finite thickness and width of teeth and slots on the dispersion behavior is also shown.**

I. Introduction

THE modal dispersion behavior of corrugated waveguides has been of interest because of their applications in structures and devices such as antennas and feeders [1], [2], mode converters [3], filters, and polarizers [4] or even in transmission systems, owing to the low attenuation characteristics that corrugated waveguides can exhibit [5], [6].

The first solutions for corrugated waveguides were based on the impedance boundary approach [7], [8]. More rigorous techniques are based on the space-harmonic formulation, i.e., a transverse field matching of the field descriptions on the different transverse regions in which the structure is decomposed [2], [9]. Other approaches are based on mode expansions on the longitudinal regions and mode matching at the transverse discontinuities of the structure [10], [11].

In this paper a mode-matching technique is presented. The use of this technique to analyze corrugated waveguides makes use of the following remarkable properties:

1) The structure alternates between large and small cross sections; hence, its discontinuities become suitable for analysis by specific multimode formulations as the admittance matrix formulation [12].
2) As a consequence of Floquet's theorem, only one spatial period must be analyzed.

The aim of this paper is to analyze corrugated waveguides by means of the mode-matching technique, a formulation with admittance multimode parameters, and the use of Floquet's theorem. The field equations and the derivation of the characteristic equation are given in Sections II and III. Section IV deals with numerical aspects (efficiency, convergence, and stability) of the proposed formulation. In Sections V and VI the method is applied to corrugated waveguides of circular and rectangular cross sections.

Manuscript received August 14, 1990; revised December 13, 1990. This work was supported by the Comisión Interministerial de Ciencia y Tecnologia (CICYT).

The authors are with the E.T.S.I. de Telecomunicación, Universidad Politénica de Madrid, Ciudad Universitaria, 28040 Madrid, Spain.

IEEE Log Number 9144282.

II. Field Equations

The geometry of one period of a general periodic corrugated structure is shown in Fig. 1, where the period has been divided into regions of smooth-walled waveguides. At both sides of each discontinuity, i.e., at $z = -t$, $z = 0$, and $z = g$, the transverse electric and magnetic fields are expanded in terms of the eigenmodes of the smooth-walled waveguides (regions I to III).

By means of current and voltage expansion coefficients [13],

$$\begin{aligned}
z = -t^+: &\quad \vec{E}_t^{IL} = \sum_n^\infty v_n^{IL}\vec{e}_n^{I} &\quad \vec{H}_t^{IL} = \sum_n^\infty i_n^{IL}\vec{h}_n^{I}\\
z = 0^-: &\quad \vec{E}_t^{IR} = \sum_n^\infty v_n^{IR}\vec{e}_n^{I} &\quad \vec{H}_t^{IR} = \sum_n^\infty i_n^{IR}\vec{h}_n^{I}\\
z = 0^+: &\quad \vec{E}_t^{IIL} = \sum_m^\infty v_m^{IIL}\vec{e}_m^{II} &\quad \vec{H}_t^{IIL} = \sum_m^\infty i_m^{IIL}\vec{h}_m^{II}\\
z = g^-: &\quad \vec{E}_t^{IIR} = \sum_m^\infty v_m^{IIR}\vec{e}_m^{II} &\quad \vec{H}_t^{IIR} = \sum_m^\infty i_m^{IIR}\vec{h}_m^{II}\\
z = g^+: &\quad \vec{E}_t^{IIIL} = \sum_n^\infty v_n^{IIIL}\vec{e}_n^{I} &\quad \vec{H}_t^{IIIL} = \sum_n^\infty i_n^{IIIL}\vec{h}_n^{I}
\end{aligned} \tag{1}$$

where the superscripts L and R denote the left and right sides of the regions, respectively.

The transverse fields $\vec{e}_n^{\nu}$ and $\vec{h}_n^{\nu}$ of the nth mode of region ν (ν = I, II, III) are suitably normalized over the cross section S_ν, so that

$$\delta_\nu(n) = \int_{S_\nu} \left(\vec{e}_n^{\nu} \times \vec{h}_n^{\nu}\right)\cdot d\vec{s} = \begin{cases} 1 & \text{for propagating modes} \\ \pm j & \text{for evanescent modes.} \end{cases} \tag{2}$$

Imposing the boundary conditions for the transverse electric and magnetic fields and using the orthogonality of

0018-9480/91/0600-0937$01.00 ©1991 IEEE

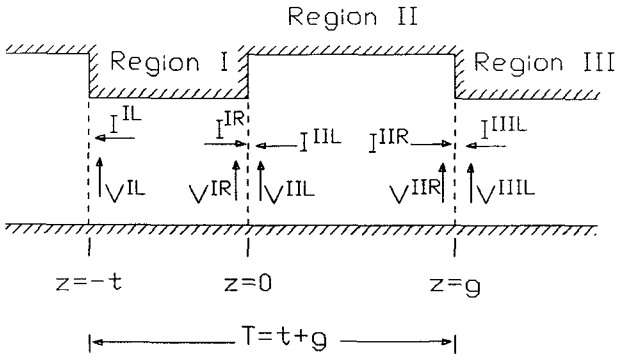

Fig. 1. Current and voltage coefficients at the discontinuities of one period of a corrugated waveguide.

the modes [14], the column vectors of current and voltage coefficients can be related to each other in the following manner. At $z = 0$,

$$\boldsymbol{V}^{\mathrm{II}L} = \boldsymbol{\Delta}_{\mathrm{II}}^{-1}\boldsymbol{S}_0^T\boldsymbol{V}^{\mathrm{I}R}$$
$$\boldsymbol{\Delta}_{\mathrm{I}}^{-1}\boldsymbol{S}_0\boldsymbol{I}^{\mathrm{II}L} = \boldsymbol{I}^{\mathrm{I}R}. \tag{3}$$

At $z = g$,

$$\boldsymbol{V}^{\mathrm{II}R} = \boldsymbol{\Delta}_{\mathrm{II}}^{-1}\boldsymbol{S}_0^T\boldsymbol{V}^{\mathrm{III}L}$$
$$\boldsymbol{\Delta}_{\mathrm{I}}^{-1}\boldsymbol{S}_0\boldsymbol{I}^{\mathrm{II}R} = \boldsymbol{I}^{\mathrm{III}L} \tag{4}$$

where $\boldsymbol{\Delta}_{\mathrm{I}}$ and $\boldsymbol{\Delta}_{\mathrm{II}}$ are diagonal matrices with elements

$$\boldsymbol{\Delta}_{\mathrm{I}} = \mathrm{diag}\left(\delta_{\mathrm{I}}(n)\right) \qquad \boldsymbol{\Delta}_{\mathrm{II}} = \mathrm{diag}\left(\delta_{\mathrm{II}}(m)\right) \tag{5}$$

and the elements of the matrix $\boldsymbol{S}_0$ are given by

$$\boldsymbol{S}_0(n,m) = \int_{S_{\mathrm{I}}} \left(\vec{e}_n^{\,\mathrm{I}} \times \vec{h}_m^{\,\mathrm{II}}\right)\cdot d\vec{s} = \boldsymbol{X}(n,m)Y_m^{\mathrm{II}}. \tag{6}$$

The matrix $\boldsymbol{S}_0$ has been decomposed, for convenience, into the product of a real and frequency-independent term, $\boldsymbol{X}(n,m)$, and the complex admittance of the mth mode of region II, Y_m^{II}.

The current and voltage coefficients in the left and right sides of region II are related by the well-known telegraphists' equation for the modes of this waveguide:

$$\boldsymbol{V}^{\mathrm{II}L} = \boldsymbol{C}_g\boldsymbol{V}^{\mathrm{II}R} + \boldsymbol{S}_g\boldsymbol{I}^{\mathrm{II}R}$$
$$\boldsymbol{I}^{\mathrm{II}L} = \boldsymbol{S}_g\boldsymbol{V}^{\mathrm{II}R} + \boldsymbol{C}_g\boldsymbol{I}^{\mathrm{II}R} \tag{7}$$

where $\boldsymbol{C}_g$ and $\boldsymbol{S}_g$ are diagonal matrices with elements

$$\boldsymbol{C}_g(m,m) = \cosh\left(\gamma_m^{\mathrm{II}}g\right)$$
$$\boldsymbol{S}_g(m,m) = \sinh\left(\gamma_m^{\mathrm{II}}g\right) \tag{8}$$

and γ_m^{II} is the propagation constant of the mth mode of region II.

Suitable manipulations of (3), (4) and (7) lead to the admittance Y-matrix representation of the combined structure (step discontinuity at $z = 0$, uniform region II, and step discontinuity at $z = g$):

$$\boldsymbol{I}^{\mathrm{I}R} = \boldsymbol{Y}_{11}\boldsymbol{V}^{\mathrm{I}R} + \boldsymbol{Y}_{13}\boldsymbol{V}^{\mathrm{III}L}$$
$$\boldsymbol{I}^{\mathrm{III}L} = \boldsymbol{Y}_{31}\boldsymbol{V}^{\mathrm{I}R} + \boldsymbol{Y}_{33}\boldsymbol{V}^{\mathrm{III}L} \tag{9}$$

where

$$\boldsymbol{Y}_{11} = \boldsymbol{Y}_{33} = -\boldsymbol{\Delta}_{\mathrm{I}}^{-1}\boldsymbol{S}_0\boldsymbol{S}_g^{-1}\boldsymbol{C}_g\boldsymbol{\Delta}_{\mathrm{II}}^{-1}\boldsymbol{S}_0^T$$
$$\boldsymbol{Y}_{13} = \boldsymbol{Y}_{31} = \boldsymbol{\Delta}_{\mathrm{I}}^{-1}\boldsymbol{S}_0\boldsymbol{S}_g^{-1}\boldsymbol{\Delta}_{\mathrm{II}}^{-1}\boldsymbol{S}_0^T. \tag{10}$$

Henceforth, the procedure used to characterize the corrugated waveguide is the same, whatever the geometry to be modeled by the Y matrices of equations (9) may be. The formulation can thus be generalized to more complex corrugated structures. However, the proposed method will be applied herein only to the simple corrugations.

As with region II, the current and voltage coefficients in the left and right sides of region I can be related by

$$\boldsymbol{V}^{\mathrm{I}R} = \boldsymbol{C}_t\boldsymbol{V}^{\mathrm{I}L} + \boldsymbol{S}_t\boldsymbol{I}^{\mathrm{I}L}$$
$$\boldsymbol{I}^{\mathrm{I}R} = \boldsymbol{S}_t\boldsymbol{V}^{\mathrm{I}L} + \boldsymbol{C}_t\boldsymbol{I}^{\mathrm{I}L} \tag{11}$$

with the definitions for $\boldsymbol{C}_t$, $\boldsymbol{S}_t$, and γ_n^{I} being similar to those of $\boldsymbol{C}_g$, $\boldsymbol{S}_g$, and γ_m^{II}.

The combination of (9) and (11) will lead to a relationship between transverse fields at the left of regions I and III, i.e., at $z = -t^+$ and $z = g^+$. But that is not the only relationship that can be stated between those fields. By means of Floquet's theorem,

$$\boldsymbol{I}^{\mathrm{III}L} = x\boldsymbol{I}^{\mathrm{I}L}$$
$$\boldsymbol{V}^{\mathrm{III}L} = x\boldsymbol{V}^{\mathrm{I}L} \tag{12}$$

where the scalar variable $x = \exp(\Gamma(t+g))$, and Γ is the propagation constant of a corrugated waveguide eigenmode (expanded, in each region, in terms of the modes of the smooth-walled waveguide that constitute that region). Since both positive and negative values of Γ are allowed, the propagation direction has not been imposed.

Equations (9), (11), and (12) lead to

$$(\boldsymbol{C}_t - \boldsymbol{Y}_{11}\boldsymbol{S}_t)\boldsymbol{I}^{\mathrm{I}L} = (-\boldsymbol{S}_t + \boldsymbol{Y}_{11}\boldsymbol{C}_t + \boldsymbol{Y}_{13}x)\boldsymbol{V}^{\mathrm{I}L}$$
$$(\boldsymbol{U}x - \boldsymbol{Y}_{13}\boldsymbol{S}_t)\boldsymbol{I}^{\mathrm{I}L} = (\boldsymbol{Y}_{13}\boldsymbol{C}_t + \boldsymbol{Y}_{11}x)\boldsymbol{V}^{\mathrm{I}L} \tag{13}$$

where $\boldsymbol{U}$ is the unit matrix.

The equation system (13) constitutes the eigenvector and eigenvalue problem, to be solved for the current and voltage coefficients and for the propagation constants of the corrugated waveguide modes.

III. The Characteristic Equation

For the numerical computation of (13), the mode sums (1) must be truncated to a finite number of terms. N_{I} modes are considered in region I (and, therefore, the same number of modes is considered in region III because of periodicity), and N_{II} modes in region II. Equations (13) lead to a characteristic equation of the form $\det(\boldsymbol{M}) = 0$, where $\boldsymbol{M}$ is a $(2N_{\mathrm{I}} \times 2N_{\mathrm{I}})$ matrix:

$$\det\begin{bmatrix} (\boldsymbol{C}_t - \boldsymbol{Y}_{11}\boldsymbol{S}_t) & (\boldsymbol{S}_t - \boldsymbol{Y}_{11}\boldsymbol{C}_t - \boldsymbol{Y}_{13}x) \\ (\boldsymbol{U}x - \boldsymbol{Y}_{13}\boldsymbol{S}_t) & -(\boldsymbol{Y}_{13}\boldsymbol{C}_t + \boldsymbol{Y}_{11}x) \end{bmatrix} = 0. \tag{14}$$

The applicable numerical root-finding methods are based on the evaluation of the determinant at a large number of values of the variable x. Since the calculation

of the determinant of an $(n \times n)$ matrix requires $\theta(n^3)$ operations, any effort to reduce the dimension of the characteristic matrix, $\boldsymbol{M}$, will have a great influence on the efficiency of the technique.

Hence, advantage can be taken of the fact that the matrix $(\boldsymbol{C}_t - \boldsymbol{Y}_{11}\boldsymbol{S}_t)$ is independent of x, in order to reduce the eigenvector dimension. From the first of equations (13), the column vector $\boldsymbol{I}^{1L}$ can be related to $\boldsymbol{V}^{1L}$, and its value can then be introduced in the second equation (13), obtaining a new eigenvalue and eigenvector problem of the form

$$(\boldsymbol{A}'x^2 + \boldsymbol{B}'x + \boldsymbol{C}')\boldsymbol{V}^{1L} = 0 \tag{15}$$

whose condition for nontrivial solution is

$$\det(\boldsymbol{A}'x^2 + \boldsymbol{B}'x + \boldsymbol{C}') = 0. \tag{16}$$

The expression (16) constitutes the new characteristic equation, where

$$\begin{aligned} \boldsymbol{A}' &= \boldsymbol{P}\boldsymbol{Y}_{13} \\ \boldsymbol{B}' &= \boldsymbol{Y}_{11} - \boldsymbol{P}(\boldsymbol{S}_t - \boldsymbol{Y}_{11}\boldsymbol{C}_t) - \boldsymbol{Y}_{13}\boldsymbol{S}_t\boldsymbol{P}\boldsymbol{Y}_{13} \\ \boldsymbol{C}' &= -\boldsymbol{Y}_{13}\boldsymbol{C}_t + \boldsymbol{Y}_{13}\boldsymbol{S}_t\boldsymbol{P}(\boldsymbol{S}_t - \boldsymbol{Y}_{11}\boldsymbol{C}_t) \end{aligned} \tag{17}$$

and

$$\boldsymbol{P} = (\boldsymbol{C}_t - \boldsymbol{Y}_{11}\boldsymbol{S}_t)^{-1}.$$

Hence, with the only drawback of the inversion of the matrix $(\boldsymbol{C}_t - \boldsymbol{Y}_{11}\boldsymbol{S}_t)$, the dimension of the characteristic matrix has been decreased from $2N_{\mathrm{I}}$ to N_{I}, with a reduction of the CPU time by a factor of $(2N_{\mathrm{I}}/N_{\mathrm{I}})^3 = 8$, i.e., almost an order of magnitude. Since $\boldsymbol{P}$ is independent of the search variable x, the calculation of $\boldsymbol{P}$ is carried out only once and does not significantly increase the computer time needed.

The matrices $\boldsymbol{A}'$, $\boldsymbol{B}'$, and $\boldsymbol{C}'$ can be scaled by premultiplying by $j\boldsymbol{\Delta}_{\mathrm{I}}$. In this manner, replacing $\boldsymbol{A}'$, $\boldsymbol{B}'$, and $\boldsymbol{C}'$ by $\boldsymbol{A} = j\boldsymbol{\Delta}_{\mathrm{I}}\boldsymbol{A}'$, $\boldsymbol{B} = j\boldsymbol{\Delta}_{\mathrm{I}}\boldsymbol{B}'$ and $\boldsymbol{C} = j\boldsymbol{\Delta}_{\mathrm{I}}\boldsymbol{C}'$ in (16), a new characteristic equation is obtained:

$$\det(\boldsymbol{A}x^2 + \boldsymbol{B}x + \boldsymbol{C}) = 0 \tag{18}$$

where the left side of the equation is a $2N_{\mathrm{I}}$-degree polynomial of real coefficients, for each of the elements of the matrix $(\boldsymbol{A}x^2 + \boldsymbol{B}x + \boldsymbol{C})$ is a two-degree polynomial with real coefficients. The $2N_{\mathrm{I}}$ roots x_{0t} of polynomial (18) give the propagation constants, $\Gamma_{0t} = \ln(x_{0i})/(t+g)$, of the different modes of the corrugated waveguide. Since no propagation direction has been imposed, both $+\Gamma_{0t}$ and $-\Gamma_{0i}$ are true propagation constants and, therefore, both x_{0i} and $1/x_{0i}$ are solutions of (18). For that reason, only N_{I} different corrugated waveguide modes are obtained, i.e., the number of summation terms in region I. This situation also arises in the analysis proposed in [10]. In addition, because of the multivalued nature of the logarithmic function, both $+\Gamma_{0i} + j2k\pi/(t+g)$ and $-\Gamma_{0t} + j2k\pi/(t+g)$ will also be roots (where k is an integer). This leads to a periodic f versus β diagram with period $2\pi/(t+g)$, as expected for a periodic structure of spatial period $T = (t+g)$.

IV. The Characterization Procedure: Numerical Aspects

The different steps of the characterization procedure can now be summarized as follows:

The first step involves computing the coupling integrals $\boldsymbol{X}(n,m)$. Given a corrugated structure, the decomposition of $\boldsymbol{S}_0$ in (6) permits the isolation of the frequency-independent integrals $\boldsymbol{X}(n,m)$ and the frequency-dependent modal admittances Y_m^{II}. In this manner, the matrix $\boldsymbol{X}$ must be computed only once, and some CPU time is saved.

The second step has two parts:

1) For each frequency, compute the matrices $\boldsymbol{A}$, $\boldsymbol{B}$, and $\boldsymbol{C}$. At first glance this computation seems to require a high number of matrix operations. However, most of the matrices involved in the formulation are diagonal. As a result, the computation of $\boldsymbol{A}$, $\boldsymbol{B}$, and $\boldsymbol{C}$ requires only six full-matrix multiplications and the inversion of matrix $\boldsymbol{P}$ that, as can easily be proved, is real.

   Furthermore, with a careful rewriting (or even with a careful coding) of the presented formulation, the utilization of complex numbers in the computation of $\boldsymbol{A}$, $\boldsymbol{B}$, and $\boldsymbol{C}$ can be avoided, since the analysis of discontinuities with admittance matrices can be carried out using real algebra [12].
2) For each frequency, solve the characteristic equation $p(x) = \det(\boldsymbol{A}x^2 + \boldsymbol{B}x + \boldsymbol{C}) = 0$. Since $p(x)$ is a $2N_{\mathrm{I}}$-degree polynomial, a quick root-finding procedure would be to sample $p(x)$ at $2N_{\mathrm{I}}$ different values x_i, then compute the coefficients of the polynomial that fits the $2N_{\mathrm{I}}$ pairs $(x_i, p(x_i))$, and then compute the roots of the fitted polynomial by means of any of the well-known algorithms. This procedure would require only $2N_{\mathrm{I}}$ evaluations of the determinant. However, this polynomial fitting technique may yield inaccurate results. If a relatively high number of terms is used, the same high number of corrugated waveguide modes will be obtained. Therefore, some computed modes will have real propagation constants with large magnitude, $\Gamma_t = \alpha_t \gg 1$, which means that for some roots $x_i = \exp(\alpha_t(t+g)) \ll 1$. Since $\Gamma_t' = -\Gamma_t$ are also correct propagation constants, for some other roots $x_t' = 1/x_t \gg 1$. Hence, $p(x)$ will have a number of roots with large magnitude, and the same number of roots with small magnitude. Sampling the polynomial to obtain its coefficients is, in this case, an unstable and inaccurate procedure. However, there is an iterative numerical root-finding technique well suited for this problem: Muller's method with implicit deflation [15]. This is a useful method for obtaining both real and complex roots of a polynomial, even if these roots are not simple. Although the method requires initial guesses, its convergence for polynomials is so good that, in fact, any initial set of guesses provides the required convergence. In any event, in the calcu-

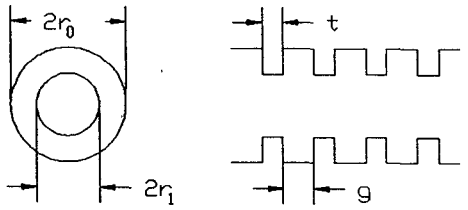

Fig. 2. Geometry of the circular corrugated waveguide.

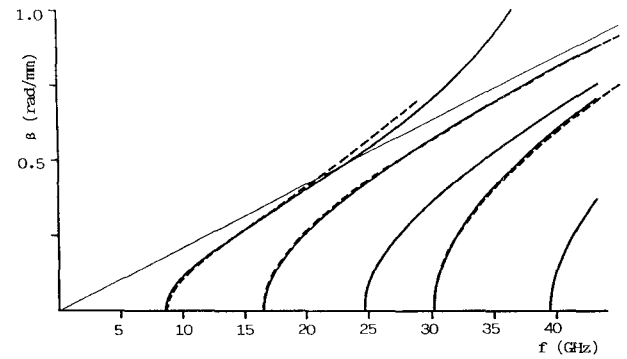

(a)

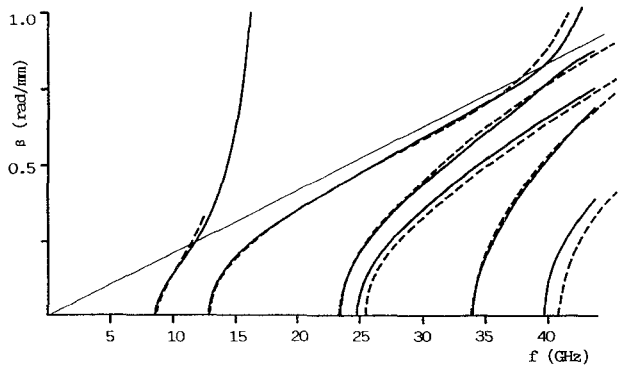

(b)

Fig. 3. Dispersion behavior of circular corrugated waveguides. $r_1 = 10.0$ mm, $t = 0.01$ mm, $g = 1.00$ mm. (a) $r_1/r_0 = 0.9$. (b) $r_1/r_0 = 0.7$. ——— Present theory. ----- Theory of [2].

lation of a Γ versus f diagram, the computed roots at a frequency f_{n-1} are excellent guesses for a frequency $f_n = f_{n-1} + \Delta f$, which speeds up the convergence rate. On the average, the computation of a Γ versus f diagram requires no more than $8N_I$ evaluations of the determinant per frequency.

The convergence of the proposed characterization technique is guaranteed by the convergence of the mode-matching technique. The relative convergence problem shown by mode-matching techniques is overcome by a suitable selection of the number of terms of the mode expansions in the different regions of the structure.

The following instability problems may arise from the utilization of the admittance matrix formulation:

- Singularities of the matrix S_g, when any of its elements $\sinh(\gamma_m^{II} g)$ vanishes. These singularities occur when $\gamma_m^{II} g = j\beta_m^{II} g = jk\pi$, for any integer k.

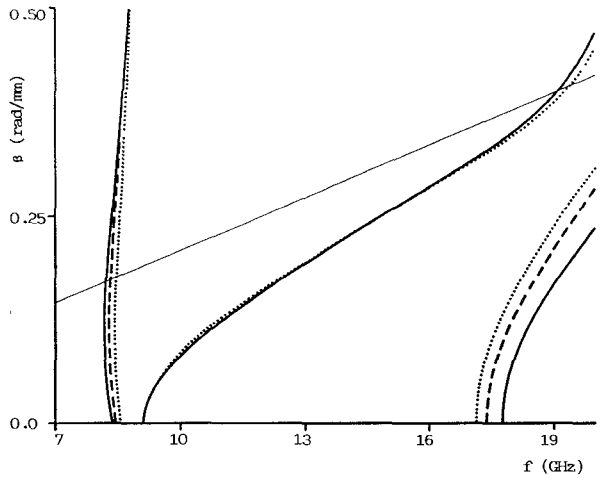

Fig. 4. Effect of finite thickness of teeth and slots. $r_1 = 10.0$ mm, $r_0 = 5.09$ mm. ——— $t = 0.01$ mm, $g = 2.0$ mm. ----- $t = 0.4$ mm, $g = 1.6$ mm. ····· $t = 0.8$ mm, $g = 1.2$ mm.

- Overflows in the computation of C_g, C_t, or S_g^{-1} when any of the values $\cosh(\gamma_m^{II} g)$, $\cosh(\gamma_n^{I} t)$, or $1/\sinh(\gamma_m^{II} g)$ is too large. These overflows occur when $\gamma_m^{II} g = \alpha_m^{II} g \gg 1$ or $\gamma_n^{I} t = \alpha_n^{I} t \gg 1$.

Nevertheless, for most of the geometries and frequency ranges of interest, the period of the structure is electrically short enough, and instabilities do not arise.

V. The Circular Corrugated Waveguide

The geometry of the circular corrugated waveguide is shown in Fig. 2. This structure has already been analyzed by different techniques, such as the wall impedance approach [7] and the space-harmonic formulation [2], with good results.

To obtain the corrugated waveguide modes with unity azimuthal dependence, only the TE_{1n} and TM_{1m} modes of the smooth-walled waveguides are required. This is due to the fact that, since the discontinuity is characterized only by a change in radii, there are no mode conversions between modes of different azimuthal dependence. The number of modes in the different regions has been selected as close as possible to the radius ratio, in order to avoid the relative convergence problem. Unless mentioned otherwise, the number of terms in the inner region (with radius r_1) is $N_1 = 10$. This number has turned out to yield sufficient asymptotic behavior.

Fig. 3 compares the results of our method with those of Clarricoats and Saha [2] for an inner radius $r_1 = 10.0$ mm and radius ratios of $r_1/r_0 = 0.9$ and $r_1/r_0 = 0.7$. Very good agreement has been obtained. It is worth remarking that the technique presented in this paper takes into account the thickness and width of teeth and slots. Hence, in order to reproduce the results of [2] (computed with the approximations $t = 0, g \ll \lambda_0$), values of t and g have been chosen so that, in the frequency range considered, $t \ll \lambda_g$ and $g \ll \lambda_g$, where λ_g is the shortest wavelength of the smooth-walled waveguides' modes. The effect of

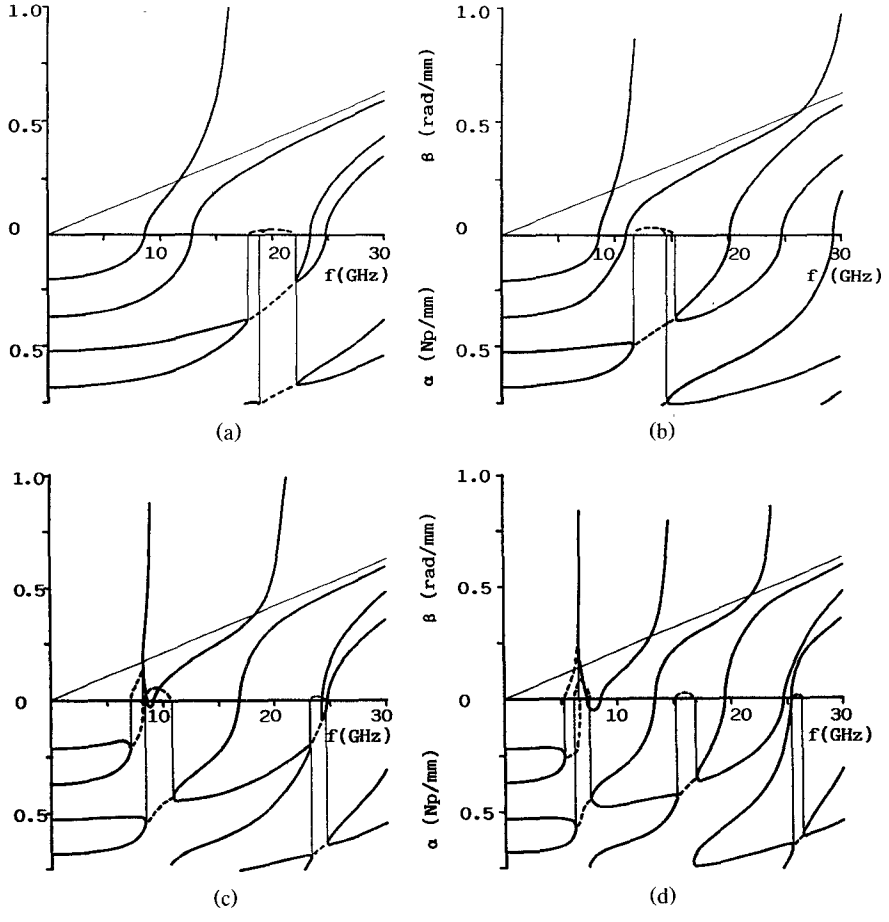

Fig. 5. Γ versus f diagrams for circular corrugated waveguides with different radius ratios. Phase and attenuation constants of complex modes are shown in dashed lines. $r_1 = 10.0$ mm, $t = 0.01$ mm, $g = 1.00$ mm. (a) $r_1/r_0 = 0.7$, (b) $r_1/r_0 = 0.6$, (c) $r_1/r_0 = 0.5$, (d) $r_1/r_0 = 0.4$.

the finite widths of slots and teeth is presented in Fig. 4 for the case $r_1/r_0 = 0.5$.

In Fig. 5, more complete Γ versus f diagrams are presented for circular corrugated waveguides with inner radius $r_1 = 10.0$ mm and different corrugation depths. For the deeper corrugations, not only normal modes are obtained, but also complex and backward-wave modes. The so-called complex modes have propagation constants with real and imaginary components (represented by dashed lines in Fig. 5), and are supported by lossless structures. These kinds of modes are known to exist in anisotropically and inhomogeneously filled waveguides [16] and have been predicted in corrugated waveguides by Cooper [17].

VI. The Rectangular Four-Corrugated-Wall Waveguide

Fig. 6 shows the geometry of a rectangular four-corrugated-wall waveguide. Although rectangular waveguides with corrugations in the broad wall alone have been successfully analyzed by the impedance boundary approach [18], in the case of corrugations on all four walls some problems arise because of the impossibility of satisfying the impedance compatibility relation [8]. More rigorous techniques have been developed for and applied to device analysis [19] and corner-filled rectangular corrugated waveguide [20].

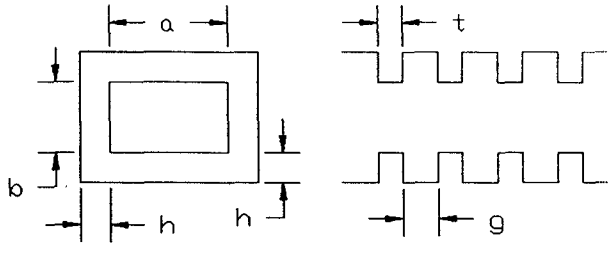

Fig. 6. Geometry of the rectangular four-corrugated-wall waveguide.

For the analysis of the four-corrugated-wall waveguide by the technique presented in this paper, and because of its symmetries, only two mode sets have been considered: (1) even modes, generated by the $TE_{m,n}$ and $TM_{m,n}$ modes of the smooth-walled rectangular waveguide with n even, and (2) odd modes, generated by $TE_{m,n}$ and $TM_{m,n}$ modes with n odd. In both cases, odd symmetry with respect to the E plane has been considered; therefore, only modes with m odd are required. The results presented in this paper have been computed by using

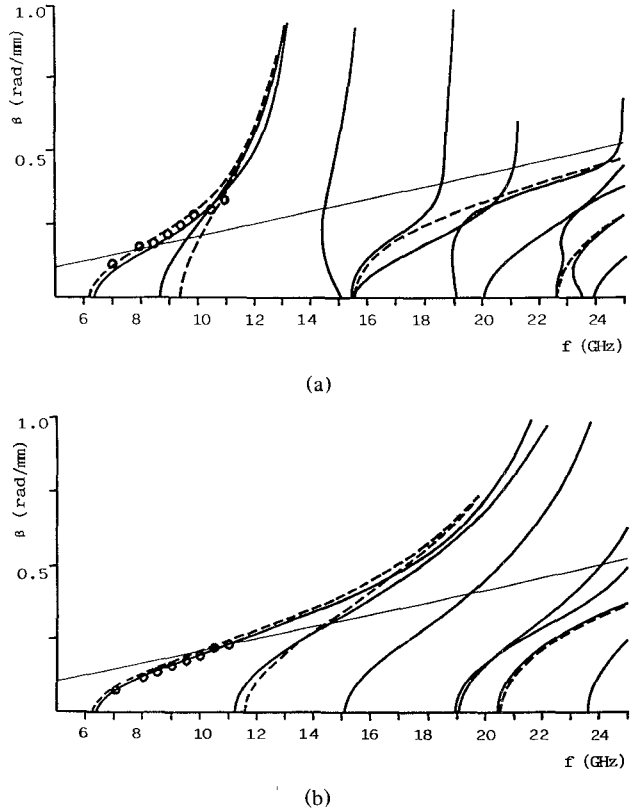

Fig. 7. Dispersion behavior of rectangular four-corrugated-wall waveguides. $a = 22.86$ mm, $b = 10.16$ mm, $t = 0.01$ mm, $g = 1.00$ mm. (a) $h = 5.08$ mm, (b) $h = 2.54$ mm. ——— Present theory. Theory (– – – –) and measurements (∘ ∘ ∘) of [21].

$N_I = 10$ terms (ten modes of the smooth-walled rectangular waveguides) in the inner regions (of cross-sectional dimensions $a \times b$). In order to avoid the relative convergence problem, in the outer region (of cross-sectional dimensions $a + 2h \times b + 2h$) the number of terms N_{II} has been chosen to keep the mode ratio N_{II}/N_I as close as possible to the area ratio $(a + 2h \times b + 2h)/(a \times b)$.

As a first test of the characterization technique presented in this paper the results presented in [21, figs. 2 and 3] have been calculated with the formulation presented herein. Once again the values of t and g have been chosen to satisfy $t \ll \lambda_g$ and $g \ll \lambda_g$. Parts (a) and (b) of Fig. 7 show, in continuous line, the modes obtained by the proposed technique for two corrugation depths (for clarity, complex modes are not shown). The crossing curves must not cause surprise, since the two independent sets of modes (with the two different symmetries) are represented in this figure. Good agreement with the theoretical and experimental results of [21] can be observed for the first two modes. However, some discrepancies have been found between the results presented in [21] and our results for higher order modes. On the one hand, our results show modes not considered in the analysis of [21]; on the other hand, the impedance model used in [21] fails to predict the transformation of higher order modes into slow waves. In Fig. 8 the significant effect of finite tooth thickness and slot width is shown.

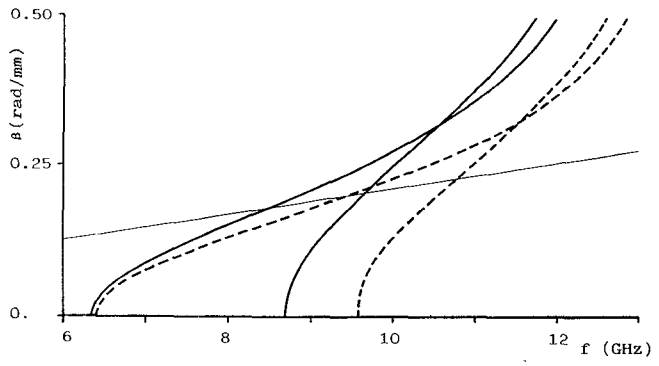

Fig. 8. Effect of finite thickness of teeth and slots. $a = 22.86$ mm, $b = 10.16$ mm, $h = 5.08$ mm. ——— $t = 0.01$ mm, $g = 1.00$ mm. – – – – $t = 1.00$ mm, $g = 2.00$ mm.

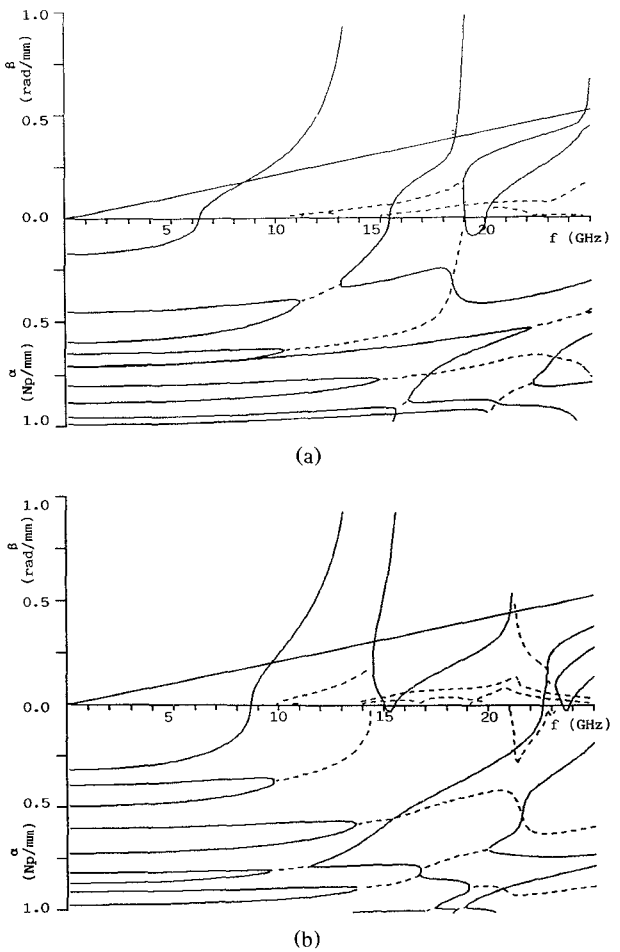

Fig. 9. Γ versus f diagrams for a rectangular four-corrugated-wall waveguide. Phase and attenuation constants of complex modes are shown in dashed lines. $a = 22.86$ mm, $b = 10.16$ mm, $t = 0.01$ mm, $g = 1.00$ mm, $h = 5.08$ mm. (a) Even modes. (b) Odd modes.

Finally, Fig. 9 shows Γ versus f diagrams for the four-corrugated-wall waveguide of Fig. 7(b). In this case, the diagrams for the two mode sets have been separated from each other. Apart from the fact that complex modes are also present in this structure, it is worth noting that these diagrams are significantly more complicated than those corresponding to circular corrugated waveguides.

VII. Conclusions

A general characterization technique for corrugated waveguides has been proposed. The technique is based on modal expansion of the fields in the smooth-walled waveguides that constitute the corrugated structure. The dispersion behavior of a corrugated structure can thus be calculated without making any assumption about tooth thickness and slot width and by taking into account all relevant geometrical parameters.

Comparisons with other techniques and experimental results have been presented, and good agreement has been obtained. The numerical examples considered include corrugated waveguides of circular and rectangular cross sections. In the rectangular case, the technique proposed in this paper yields more accurate predictions of the higher order modes than those based on the wall impedance approach. In both circular and rectangular geometries, and for deep corrugations, complex modes have been obtained, as previously suggested by other authors.

References

[1] H. C. Minnet and B. MacA. Thomas, "A method of synthesizing radiation patterns with axial symmetry," *IEEE Trans. Antennas Propagat.*, vol. AP-14, pp. 654–656, 1966.

[2] P. J. B. Clarricoats and P. K. Saha, "Propagation and radiation behaviour of corrugated feeds," *Proc. Inst. Elec. Eng.*, vol.-118, pt. H., no. 9, pp. 1167–1176, Sept. 1971.

[3] G. L. James, "Analysis and design of TE_{11}-to-HE_{11} corrugated cylindrical waveguide mode converters," *IEEE Trans. Microwave Theory Tech.*, vol. MTT-29, pp. 1059–1066, 1981.

[4] F. Arndt, W. Tucholke, and T. Wriedt, "Broadband dual-depth *E*-plane corrugated square waveguide polariser," *Electron. Lett.*, vol. 20, no. 11, pp. 458–459, May 1984.

[5] A. M. B. Al-Hariri, A. D. Olver, and P. B. J. Clarricoats, "Low-attenuation properties of corrugated rectangular waveguide," *Electron. Lett.*, vol. 10, no. 15, pp. 304–305, July 1974.

[6] C. Dragone, "Attenuation and radiation characteristics of the HE_{11}-mode," *IEEE Trans. Microwave Theory Tech.*, vol. MTT-28, pp. 704–710, July 1980.

[7] C. Dragone, "Characteristics of a broadband microwave corrugated feed: A comparison between theory and experiment," *Bell Syst. Tech. J.*, vol. 56, no. 6, pp. 869–888, July–Aug. 1977.

[8] R. Dybdal, L. J. Peters, and W. H. Peake, "Rectangular waveguides with impedance walls," *IEEE Trans. Microwave Theory Tech.*, vol. MTT-19, pp. 2–9, Jan. 1971.

[9] A. D. Olver, K. K. Yang, and P. J. B. Clarricoats, "Propagation and radiation behaviour of dual-depth corrugated horns," *Proc. Inst. Elec. Eng.*, vol. 131, pt. H, no. 3, pp. 179–185, June 1984.

[10] R. E. Collin, *Field Theory of Guided Waves*. New York: McGraw-Hill, 1961, pp. 390–401.

[11] K. A. Zaki and S. W. Chen, "Periodically loaded dielectric waveguides," in *Proc. IEEE AP-S Int. Conf.* (Syracuse, NY), June 1988, pp. 560A–563.

[12] F. Alessandri, G. Bartolucci, and R. Sorrentino, "Admittance matrix formulation of waveguide discontinuity problems: Computer-aided design of branch guide directional couplers," *IEEE Trans. Microwave Theory Tech.*, vol. 36, pp. 394–403, Feb. 1988.

[13] N. Marcuvitz, *Waveguide Handbook*. New York: Mc-Graw Hill, 1951, p. 5.

[14] R. E. Collin, *Field Theory of Guided Waves*. New York: McGraw-Hill, 1961, p. 174.

[15] J. F. Traub, *Iterative Methods for the Solution of Equations*. Englewood Cliffs, NJ: Prentice-Hall, 1964, pp. 210–213.

[16] A. S. Omar and K. F. Schünemann, "Complex and backward-wave modes in inhomogeneously and anisotropically filled waveguides," *IEEE Trans. Microwave Theory Tech.*, vol. MTT-35, pp. 268–275, Mar. 1987.

[17] D. N. Cooper, "Complex propagation coefficients and the step discontinuity in corrugated cylindrical waveguide," *Electron. Lett.*, vol. 7, nos. 5/6, pp. 135–136, Mar. 1971.

[18] R. Baldwin and P. A. McInnes, "Corrugated rectangular horns for use as microwave feeds," *Proc. Inst. Elec. Eng.*, vol. 122, no. 5, pp. 465–469, May 1975.

[19] E. Khün and B. K. Watson, "Rectangular corrugated horns—analysis, design and evaluation" in *Proc. 14th European Microwave Conf.* 1984, pp. 221–227.

[20] L. C. Da Silva and S. Ghosh, "A comparative analysis between rectangular corrugated waveguides with plain and corner filled corrugations," in *Proc.* 1990 *AP-S Symp.* (Dallas), pp. 976–979.

[21] A. A. S. Obaid, T. S. M. Maclean, and M. Razaz, "Propagation characteristics of rectangular corrugated waveguides," *Proc. Inst. Elec. Eng.*, vol. 132, pt. H., no. 7, pp. 413–418, Dec. 1985.

Jaime Esteban was born in Madrid, Spain, in 1963. He received the Ingeniero de Telecomunicación and Ph.D. degrees, both from the Universidad Politécnica de Madrid, Spain, in September 1987 and July 1990, respectively.

From January 1988 to October 1990 he was with the Grupo de Electromagnetismo Aplicado y Microondas at the Universidad Politécnica de Madrid working on numerical methods for electromagnetism through a scholarship from the Spanish Ministry of Education and Science. He is currently Assistant Professor in the Departamento de Electromagnetismo y Teoría de Circuitos, Universidad Politécnica de Madrid. His research interests include analysis and design of microwave and millimeter-wave devices, analysis and characterization of waveguides and transmission lines, and planar structures.

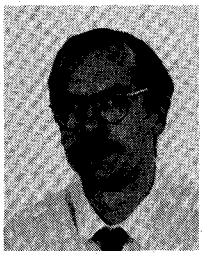

Jesús M. Rebollar was born in Beasain (Guipuzcoa), Spain, in 1953. He received the Ingeniero de Telecomunicación degree in 1975 and the Ph.D. degree in 1980, both from the Universidad Politécnica de Madrid, Spain.

Since 1976 he has been with the Grupo de Electromagnetismo Aplicado y Microondas at the Universidad Politécnica de Madrid, as Assistant Professor (1977–1982) and Associate Professor (1982–1988). In 1988, he was appointed Professor of Teoría Electromagnética. His current research interests are electromagnetic wave propagation in waveguide structures, interactions of electromagnetic fields with biological tissues, and particularly CAD for microwave and millimeter-wave passive devices.